JOURNAL OF GEOPHYSICAL RESEARCH, VOL. 94, NO. B9, PAGES 12,363–12,374, SEPTEMBER 10, 1989

Centroid Single Force Inversion of Seismic Waves Generated by Landslides

HITOSHI KAWAKATSU[1]

Seismological Laboratory, California Institute of Technology, Pasadena

The centroid moment tensor (CMT) waveform inversion method of Dziewonski et al. (1981) is modified to analyze long period seismic waves generated by "single force" events such as the gigantic landslides associated with the 1980 eruption of Mount St. Helens. We refer to the method as centroid single force (CSF) inversion. As the result of the inversion we obtain the spatio-temporal centroid and three components of a vector we call the CSF vector, which is the seismic point source representation of a landslide and whose direction is the opposite of the direction of sliding. The scaler magnitude of the CSF vector measures the overall size of the landslide and is given by $M_{CSF} = MD$, where M is the mass of the sliding object and D is the sliding distance. We apply CSF inversion to the long period surface waves generated by the 1980 Mount St. Helens event, the 1975 Kalapana earthquake, and the 1974 Mantaro landslide, using seismograms from the GDSN, IDA and HGLP networks. The CSF solution for the St. Helens event is remarkably consistent with the actual geological observations and proves the efficacy of CSF inversion. The CSF solution for the Kalapana event does not fit the overall waveforms better than the CMT solution does. However, because the CMT solution does not explain the observed Love wave radiation pattern, it may be necessary to invoke a combination of both types of mechanism for this event. Although the geometry of the CSF solution (the direction of the force) for the Mantaro event is consistent with the actual landslide, M_{CSF} is about 5 times smaller than that expected from the mass and travel distance of the landslide estimated by geological observations. This discrepancy may suggest either the relatively aseismic nature of this landslide or that the total volume of the slide was overestimated. By analogy to single station CMT inversion, single station CSF inversion also appears to be stable and useful.

INTRODUCTION

The advent of high quality digital seismic networks, together with recent developments in theoretical seismology has led to great progress in seismic source mechanism studies. For example, source mechanisms of earthquakes are now routinely determined by analyzing seismic waveforms, and hundreds of new reliable solutions are obtained every year [e.g, *Dziewonski et al.*, 1981; *Sipkin*, 1986]. It is now even possible to obtain earthquake source mechanisms in a quasi-real-time manner by analyzing waveforms from a few broad-band instruments [*Ekström et al.*, 1986], and real-time analysis of seismic events using waveforms may become possible in the near future.

The high sensitivity and quality of digital network data have also helped to convincingly identify some non-fault type "earthquakes." Kanamori, in a series of papers with his coworkers, has shown that massive landslides (both subaerial and submarine) may generate long period seismic waves comparable in amplitude to major earthquakes, and has suggested that some large earthquakes, which had been believed to have a double-couple mechanism, might instead have had a so-called single-force mechanism (the kinematic seismic source equivalent of a landslide) [*Kanamori and Given*, 1982; *Kanamori et al.*, 1984; *Eissler and Kanamori*, 1987; *Hasegawa and Kanamori*, 1987]. Source mechanisms of such non-fault earthquakes cannot be parameterized by either a conventional double-couple or a moment tensor. In order to perform routine waveform analysis of earthquakes including such events, a new parametrization scheme is essential.

In this paper we extend the centroid moment tensor (CMT) waveform inversion method (developed by *Dziewonski et al.* [1981] and *Dziewonski and Woodhouse* [1983]) to analyze long period seismic waves generated by such "single force" events. We will show that the momentum of the sliding object (rather than the seismic moment rate) should be used as the source time function, and that the seismic point source representation of a landslide is a vector whose magnitude is the product of the mass and the travel distance of the slide. We call this method centroid single force (CSF) inversion and apply it to the 1980 Mount St. Helens event, the 1975 Kalapana event, and the 1974 Mantaro landslide. The method is quite stable; it is even possible to estimate the main features of landslides from single station data.

There may exist many seismic events like landslides (especially submarine landslides) which have a long source time duration. Such events can be sometimes overlooked by conventional "first motion" seismology, which is based on high frequency data. Analyzing waveform data obtained from global digital seismic networks using methods such as CMT inversion [*Dziewonski et al.*, 1981] and CSF inversion may reveal new types of seismic events, which might have been overlooked.

CENTROID SINGLE FORCE INVERSION

Since the derivation of the centroid single force inversion method is essentially the same as that of centroid moment tensor inversion of *Dziewonski et al.* [1981] and *Dziewonski and Woodhouse* [1983], we briefly note the differences here (see also Appendix B).

Figure 1 schematically illustrates the differences of source time functions of an earthquake faulting and a landslide. In the case of an earthquake faulting, it is the spatial derivative of a moment tensor density (or a stress glut [*Backus and Mulcahy*, 1976]) which enters into the equation of motion. As a physically meaningful source function we have a seismic moment (Figure 1a). As a teleseismic source time function, we usually use the moment rate function, which is expected to be a one-sided function during the faulting (Figure 1b). Then we may

[1]Now at Geological Survey of Japan, Tsukuba, Ibaraki, Japan.

Copyright 1989 by the American Geophysical Union.

Paper number 89JB01118.
0148-0227/89/89JB-01118$05.00

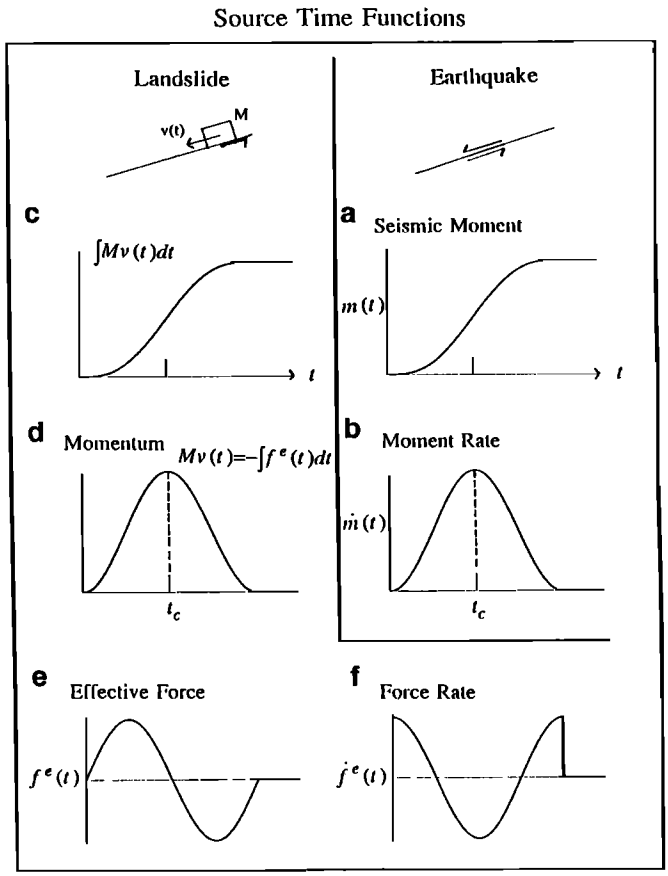

Fig. 1. A schematic figure to compare source time functions of an earthquake (fault) source and a landslide. Note that the time integral of the momentum of the sliding object has a characteristic similar to the moment function of an earthquake.

take the centroid of the moment rate to represent the temporal centroid of the event. The integral of the moment rate is the total moment which should represent the physical size of the earthquake. In the case of a landslide, it is the effective force which enters into the equation of motion. The effective force is the difference between the force initially exerted to the Earth by the sliding object and the force exerted during the slide. The positive part corresponds to the acceleration stage of the slide and the negative one to the deceleration stage (Figure 1e). If we use a simple-minded analogy from the earthquake faulting, we may take a force rate as a source time function (Figure 1f). However, neither the force rate nor the force function itself has a such nice one-sided character as the moment rate and their integrals are expected to be zero. This means that if we use the simple-minded analogy, we may try to obtain a solution which is expected to be zero. Instead the time integral of the effective force function, which is the negative of the momentum of the sliding object (Figure 1d), should be used as a source time function to define a temporal centroid. Noticing these differences, it is straightforward to modify the CMT method to analyze landslides. The physical quantity which should represent a size of a landslide is the integral of the momentum and turns out to be a mass of the landslide multiplied by its traveling distance. Considering these basic differences between an earthquake faulting and a landslide, we will derive the CSF inversion method in the following.

Force Equivalent of a Landslide

The kinematic equivalence of a landslide and a "single force" system is described in a series of papers by Kanamori and his co-workers [*Kanamori and Given*, 1982; *Kanamori et al.*, 1984; *Eissler and Kanamori*, 1987; *Hasegawa and Kanamori*, 1987]. We assume that as far as the excitation of long period seismic waves is concerned, a landslide can be represented by the sliding of a block on a slope as shown in Figure 1. We define the contact (surface) force exerted on the Earth by the sliding object as $\mathbf{f}(\mathbf{x},t)$. Before and after the event, this force ($\mathbf{f}(\mathbf{x},0)$ or $\mathbf{f}(\mathbf{x},\infty)$) is constant (i.e., the whole system is in a static state) and its spatial integral is equal to the total gravitational force exerted on the object by the Earth. During the event there is a redistribution of the force system both in space and time, but the total force system is constant, i.e.,

$$\int_{E_S} \mathbf{f}(\mathbf{x},0)dS = \int_{E_S} \mathbf{f}^a(\mathbf{x},t)dS + \int_O m(\mathbf{x},t)\alpha(\mathbf{x},t)dV = \text{const} \quad (1)$$

where $\mathbf{f}^a(\mathbf{x},t)$ denotes the surface force actually exerted on the Earth by the slide, and $m(\mathbf{x},t)$ and $\alpha(\mathbf{x},t)$ are the mass per unit volume (i.e., density) and acceleration of the sliding object, respectively. The integration is done on the surface of the Earth (E_s) where the landslide takes place and over the entire volume of the landslide (O). Assuming that the wavelength of the seismic wave is much longer than the spatial extent of the landslide, we may rewrite the above equation as

$$\mathbf{F}(t) = \mathbf{F}^a(t) + M\alpha(t) = \text{const} \quad (2)$$

where capital letter quantities are the spatial integrals of the corresponding lower case quantities. The effective force which excites seismic waves may then be defined as

$$\mathbf{F}^e(t) \equiv \mathbf{F}^a(t) - \mathbf{F}(0) = -M\alpha(t) \quad (3)$$

The direction of this force is the opposite of the direction of the landslide. The time integral of the effective force,

$$\mathbf{P}(t) \equiv \int_0^t \mathbf{F}^e(t)dt = -M\int_0^t \alpha(t)dt = -M\mathbf{v}(t) \quad (4)$$

is the negative of the momentum of the sliding object at time t. It is obvious that after a certain time has passed the sliding object has to stop (unless it has become completely detached from the Earth) and that the momentum has to become zero, i.e., $\mathbf{P}(\infty) = 0$. The time integral of $\mathbf{P}(t)$ is

$$\int_0^\infty \mathbf{P}(t)dt = -M\,\mathbf{D} \equiv \mathbf{P}^{(0,0)} \quad (5)$$

where $\mathbf{D}$ is a vector which connects the initial and final centroids of the sliding object.

Normal Mode Excitation

Following *Gilbert and Dziewonski* [1975] and *Dziewonski and Woodhouse* [1983], using normal mode summation we may write the seismic displacement in a spherically symmetric Earth model excited by a force $\mathbf{f}(\mathbf{x},t)$ as

$$\mathbf{s}(\mathbf{x},t) = \sum_k a_k(t)\mathbf{u}_k(\mathbf{x}) \quad (6)$$

where $\mathbf{u}_k(\mathbf{x})$ is a normalized eigenfunction of the spherically symmetric Earth model (in the present paper we use model 1066A of *Gilbert and Dziewonski* [1975] and $a_k(t)$ is the excitation function of mode k, and may be written as

$$a_k(t) = \frac{1}{\omega_k}\int_{-\infty}^{t} \sin\omega_k(t-t')\Gamma_k(t')dt' \quad (7)$$

where

$$\Gamma_k(t) = \int u_k^*(x)\cdot f(x,t)dV \quad (8)$$

In the case of earthquake sources we usually rewrite (7) by integrating by parts:

$$a_k(t) = \frac{1}{\omega_k^2}\int_{-\infty}^{t} (1-\cos\omega_k(t-t'))\dot{\Gamma}_k(t')dt' \quad (9)$$

In the case of landslides, however, for a reason which will become clear later, we rewrite (7) as

$$\begin{aligned} a_k(t) &= \int_{-\infty}^{t} \cos\omega_k(t-t')\int^{t'} \Gamma_k(\tau)d\tau dt' \\ &= \int_{-\infty}^{t} \cos\omega_k(t-t')\int u_k^*(x)\cdot p(x,t')dx^3dt' \end{aligned} \quad (10)$$

where

$$p(x,t) = \int_0^t f(x,\tau)d\tau \quad (f(x,t)=0 \text{ for } t<0) \quad (11)$$

which may be called the negative of the momentum density.

In order to define the centroid of the landslide, we exactly follow the treatment proposed by *Dziewonski et al.* [1981] and *Dziewonski and Woodhouse* [1983] for earthquakes. Following *Backus* [1977], we define the centroid of the vector field $\mathbf{p}(x,t)$ as the point about which the sum of square of the first moments is minimum. Expanding (10) at some fiducial point (x_s,t_s), the excitation function may be written as

$$\begin{aligned} a_k(t) \approx\ & h_k(t-t_s)[P_i^{(0,0)}(u_i^*+\Delta x_p u_{i,p}^*) + P_{ip}^{(1,0)}(x_c)u_{i,p}^*] \\ & - \dot{h}_k(t-t_s)[\Delta t P_i^{(0,0)}+P_i^{(0,1)}(t_c)]u_i^* \end{aligned} \quad (12)$$

where

$$\begin{aligned} h_k(t) &= \cos\omega_k t\, e^{-\alpha_k t} \\ P_i^{(0,0)} &= \int_{-\infty}^{\infty}dt'\int_{vs}dx^3 p_i(x,t') \\ P_{ip}^{(1,0)}(x_s) &= \int_{-\infty}^{\infty}dt'\int_{vs}dx^3(x_p-x_{sp})p_i(x,t') \\ P_i^{(0,1)}(t_s) &= \int_{-\infty}^{\infty}dt'\int_{vs}dx^3(t-t_s)p_i(x,t') \\ \Delta x &= x_c - x_s \\ \Delta t &= t_c - t_s. \end{aligned} \quad (13)$$

Neglecting the first-moment contributions, which are minimum in the least square sense at the centroid, we get an expression for the seismic displacement field of the form

$$s_i(x,t) = \sum_{j=1}^{3}\psi_{ij}(t)P_j + \delta r_s b_i(t) + \delta\theta_s c_i(t) + \delta\phi_s d_i(t) + \Delta t e_i(t) \quad (14)$$

where $\psi_{ij}(t)$, $b_h(t)$, $c_h(t)$, $d_h(t)$, $e_h(t)$ are obtained by summation over all modes and i=1,2,3 denote the vertical, radial and transverse components, respectively. The explicit form of the terms in (14) is given in Appendix B. $\mathbf{P}^{(0,0)} = (P_1^{(0,0)}, P_2^{(0,0)}, P_3^{(0,0)})$ is the "centroid single force vector," which is the point source representation of a landslide event. The direction of this vector is the opposite of the direction of sliding (from (4) and (5)). Although the term 'CSF' contains the word 'force,' the actual dimension of the CSF vector is not that of force but rather (Mass)×(Distance) (see equation (5)). The absolute value of the CSF vector will be called the "CSF value (M_{CSF})" in the following discussions, and it represents the overall size of the landslide; $M_{CSF} = M\cdot D$.

It should be now clear why we use (10), rather than (7) and (9). From the natural requirement that the sliding object has to stop sometime, the spatial and time integral of both the effective (single) force and the force rate have to become zero. Therefore the zeroth moment of those quantities is zero, and it is difficult to define a centroid. Equation (14) forms the basis for iterative inversion for the simultaneous determination of the single force vector and the centroid location from waveform data. The rest of the inversion procedure precisely follows that of *Dziewonski et al.* [1981] and *Dziewonski and Woodhouse* [1983].

APPLICATIONS

Mount St. Helens, May 18, 1980

We first apply the CSF inversion method to the long period surface waves generated by the landslide associated with the May 18, 1980 eruption of Mount St. Helens. This event was well studied and documented by many researchers [e.g., *Voight et al.*, 1981; *Kanamori and Given*, 1982; *Kanamori et al.*, 1984; *Burger and Langston*, 1985] and thus is useful as a test for the CSF inversion method.

The data are obtained from the GDSN and IDA networks; the station coverage is shown in Figure 2. Each seismogram is deconvolved with an appropriate instrument response and band-pass filtered between 4 and 5 mHz. We use three component (vertical, radical, and transverse) seismograms which usually contain the first two successive surface wave trains (the average record length is about 9000 seconds).

Figures 3 and 4, and Table 1 summarize the results of the CSF inversion. Figure 3 shows an equal area projection of the unit focal sphere. Each symbol represents a CSF vector of unit length. Open and solid symbols denote points on the upper and lower hemisphere, respectively. The star indicates the CSF solution obtained by inverting all the available waveforms. The arrow shows the location of the centroid relative to the location of a m_b = 4.7 (M_s = 5.2) earthquake reported by the National Earthquake Information Service (NEIS) (hypocenter: 46.214° N,

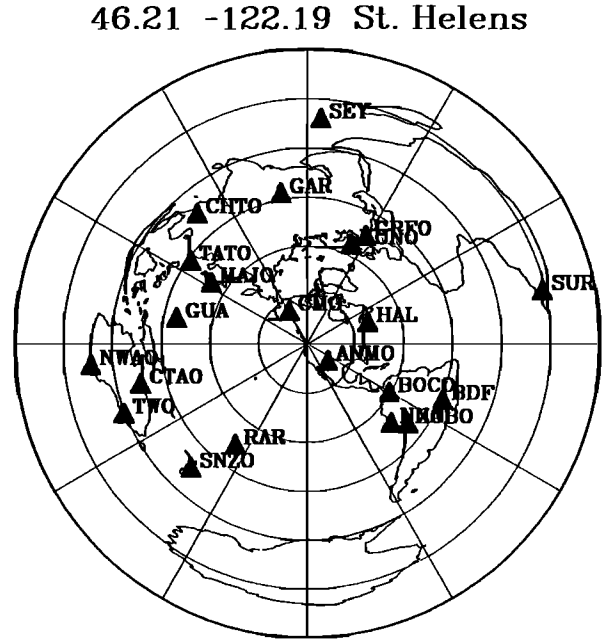

Fig. 2. The station coverage for the Mount St. Helens event.

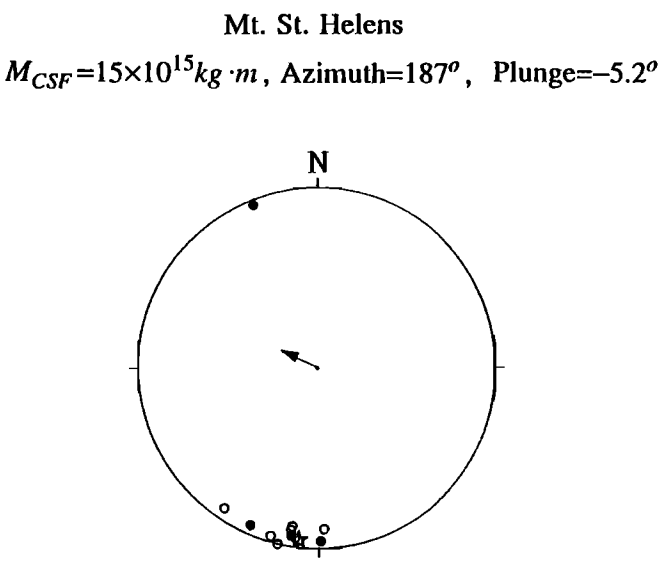

Fig. 3. Equal area projection of CSF solutions for the St. Helens event. The star indicates the full data set CSF solution. The circles denote single station solutions. Open and solid symbols are on the upper and the lower hemisphere, respectively. The arrow shows the centroid location shift of the CSF solution, and the radius of the outer circle corresponds to 1°.

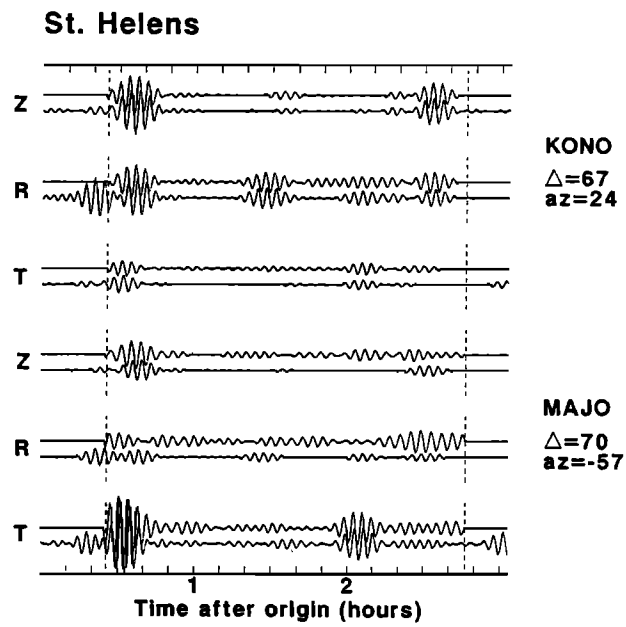

Fig. 4. Comparison of observed and synthetic seismograms at KONO and MAJO for St. Helens event. For each pair of seismograms, the top and bottom traces are the observed and synthetic seismograms. For each station, the top, middle, and bottom seismograms are vertical, radial, and transverse components, respectively. The vertical dashed lines indicate the time windows used for the inversion. The tick marks are for every 10 minutes.

122.194° W, origin time 1532:11 UT, May 18, 1980). The radius of the outer circle is 1° in this case. Circles are the solutions of the single station inversion. Single station CSF inversion is performed for all the stations which have three components seismograms (i.e., GDSN stations). Following *Ekström et al.* [1986], we constrain the spatial centroid to be located on the great circle which connects the source and the station.

The CSF solution with the full data set indicates that the direction of the force is 7° west of south. This is consistent with the result of *Kanamori and Given* [1982] and with the observed direction of the landslide. The CSF vector plunge is 5.2° (±2°) upward and slightly smaller than that of *Kanamori and Given* [1982].

The CSF value of 1.5×10^{16} (kg m) should be multiplied by 1.54 to correct for the effect of source finiteness. We assume a sinusoidal source time function as shown in Figure 1e and use a half duration of 90 s, after *Kanamori et al.* [1984]. The choice of a particular source time function does not change the correction value more that a factor of 0.5 and we use the sinusoidal source time function in the rest of the paper. The static (zero frequency) CSF value is, then, 2.2×10^{16} (kg m). As mentioned in the previous section, the CSF value corresponds to the mass of the slide times the sliding distance (equation (5)). If we take the mass of the slide to be 4.6×10^{12} kg [*Kanamori and Given*, 1982], we get a sliding distance of 4.8 km. According to *Voight et al.* [1981], the centroid of the rockslide-avalanche traveled a horizontal distance of about 5 km northward until it reached a point near Spirit Lake, from where the main lobe funneled westward along the North Fork Toutle River valley. Therefore, if we consider that from long period surface waves (period of ~225 s) we are observing the northward movement of the landslide, the CSF solution is quite consistent with the actual phenomenon.

In terms of the force time history, if we assume a sinusoidal force time function with a half duration of 90 s [*Kanamori et*

TABLE 1. CSF Solutions (4-5 mHz) for Mount St. Helens

Data	M_{CSF} (10^{15} kg m)	Azimuth, deg	Plunge, deg	Centroid Latitude, deg	Centroid Longitude, deg	Time, s
All	14.6±0.7	186.7±02.6	-5.2±01.8	+0.09	-0.20	103.3
ANMO	18.3±1.7	196.1±07.7	-3.7±06.8	-0.06	+0.11	111.3
BCAO	19.2±8.1	338.5±16.4	3.5±10.2	0.27	0.40	66.8
BOCO	16.9±3.4	189.4±14.9	6.6±12.5	0.01	-0.02	109.3
CHTO	18.8±2.9	193.3±10.0	0.0±08.4	-0.18	0.21	114.6
CTAO	11.6±2.2	189.5±07.6	-12.1±05.1	0.12	0.73	79.3
GRFO	19.7±3.9	179.3±07.7	4.5±08.8	0.14	0.11	109.1
KONO	13.6±1.0	186.7±04.9	-4.2±02.9	0.09	0.06	104.0
MAJO	15.0±2.4	188.0±09.2	-5.4±06.9	0.11	-0.25	105.9
NWAO	15.5±1.7	189.8±07.5	-9.9±06.9	-0.04	-0.62	88.2
SNZO	12.7±4.1	214.2±44.7	-6.9±11.1	-0.02	-0.03	95.4
TATO	26.7±9.8	178.0±22.1	-11.6±19.7	-0.03	0.07	110.4
ZOBO	11.1±1.9	203.6±08.1	5.6±05.7	-0.06	1.23	87.9

Centroid location is relative to 46.214°N, –122.194°E, and centroid time is relative to 1532:11.0, reported by NEIS.

al., 1984] our CSF solution translates into a peak force of 0.42×10^{13} N. This value appears to be slightly smaller than that of *Kanamori et al.* [1984] (it should be compared with their Figure 15) on the average, but the difference does not seem to be significant.

The Centroid Moment Tensor inversion method of *Dziewonski et al.* [1981] was also applied to the same dataset, but no appropriate solution was obtained. When the depth is allowed to move, CMT inversion converged to a centroid deeper than 100 km and about 3.5° away from the location of Mount St. Helens. When the depth is fixed at 10 km, the CMT solution gives a pure dip slip mechanism with an almost horizontal fault plane. Although this mechanism can generate a two-lobe pattern for the Love wave radiation, the centroid is shifted by more than 2° (~ 200 km).

Kalapana, Hawaii, November 29, 1975

The mechanism of the Ms=7.1, November 29, 1975, Kalapana earthquake has been controversial. *Ando* [1979] and *Furumoto and Kovach* [1979] suggested a double couple mechanism with a nearly horizontally dipping fault plane at a depth of about 10 km. The estimated seismic moments range from 1.2×10^{20} N m [*Furumoto and Kovach*, 1979] to 1.8×10^{20} N m [*Ando*, 1979]. Recently, *Eissler and Kanamori* [1987] proposed a single force mechanism for the generation of long-period surface waves, similar to that for the Mount St. Helens event, but *Wyss and Kovach* [1988] argue for a nearly horizontal thrust faulting. It is therefore worthwhile to reexamine this event using CSF inversion to see whether or not a single force model is required by the data.

We have obtained data from two IDA stations and six digital HGLP stations, whose distribution is shown in Figure 5. Since the first surface wave arrivals (G1 and R1) are off scale for this event, we use the portion of the seismograms which contains G2, G3, R2, and R3 wave trains. Each seismogram is deconvolved with an appropriate station response (see Appendix A for the HGLP station response) and filtered between 4 and 5 mHz.

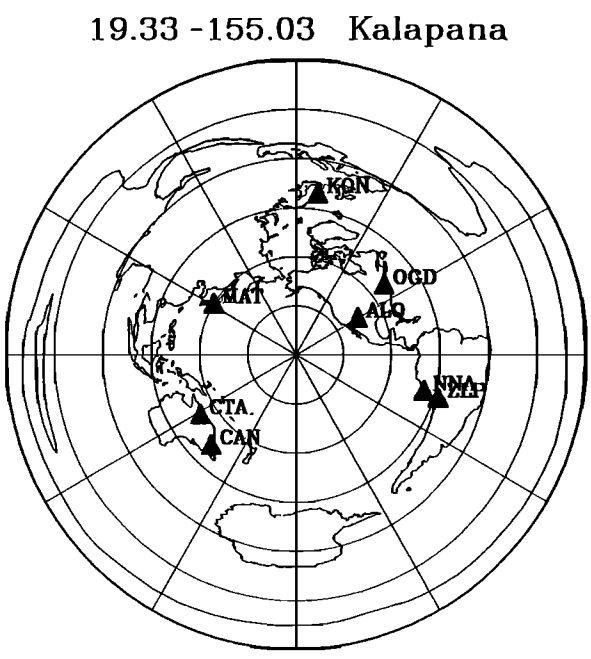

Fig. 5. The station coverage for the Kalapana event.

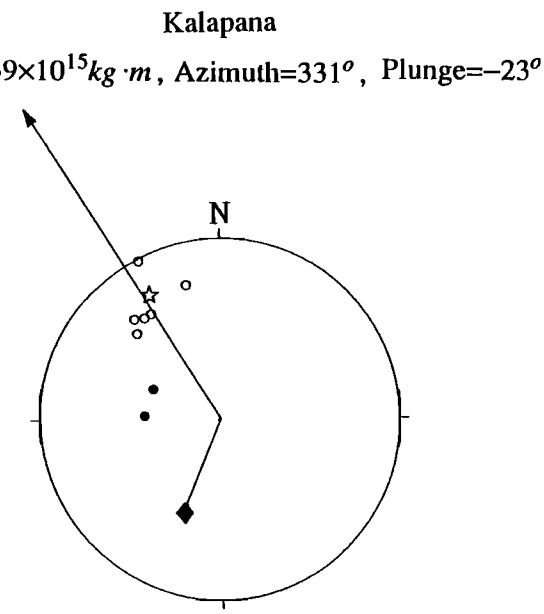

Fig. 6. Same as Figure 3 but for the Kalapana event. The diamond symbol indicates the centroid shift of the CMT solution.

Figures 6 and 7, and Table 2 summarize the result of the CSF inversion.

The CSF solution with the full data set indicates that the direction of the force is 29° west of north. This is consistent with the result of *Eissler and Kanamori* [1987] and with the observed direction of the movement of the south flank of Kilauea [*Lipman et al.*, 1985].

The source finiteness correction for the CSF value 3.4×10^{17} kg m should be less than 10%, since the half duration of the source is between 30 and 40 s (H. Kawakatsu and H. Kanamori, manuscript in preparation, 1989). The static (zero frequency) CSF value is, then, about 3.7×10^{17} kg m which is 17 times larger than that of Mount St. Helens. If we take the mass to be 10^{15}-10^{16} kg [*Eissler and Kanamori*, 1987], we get a sliding distance of between 37 and 370 m. These values are about seven times smaller than those suggested by *Eissler and Kanamori* [1987]. In terms of the force time history, if we assume a sinusoidal force time function with a half duration of 40 s, our CSF solution translates into a peak force of 3.3×10^{14} N. This value is about 3 times smaller than that of *Eissler and Kanamori* [1987]. A part of these discrepancies is due to the fact that *Eissler and Kanamori* assumed the half duration of 90 s when they estimated the peak force from the Love wave amplitudes at ~ 100 s, while we think the half duration is about 40 s.

Although there may be some significant differences in the absolute force size between the CSF solution and Eissler and Kanamori's result, the geometry of the solutions is quite similar. It appears, therefore, that the Kalapana event can be well explained by a single force model similar to that for the Mount St. Helens event proposed by *Eissler and Kanamori* [1987]. However, the Kalapana earthquake is different from the St. Helens event in the following points, and does not appear to be simply explainable by a single force model.

The CMT inversion applied to the Kalapana data set converges to the solution shown in Table 3 and Figure 8. The CMT solution is quite reasonable in the sense that the best double couple solution [*Dziewonski et al.*, 1981] is close to that of

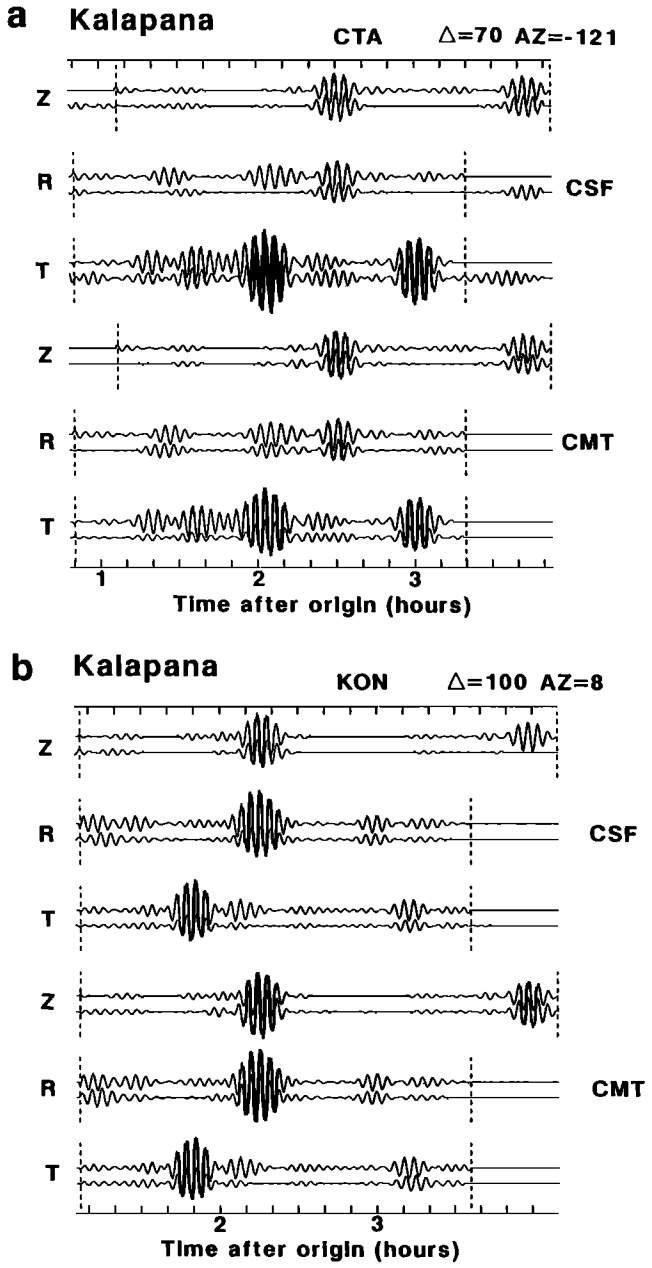

Fig. 7. Similar to Figure 4. Comparison of observed and synthetic seismograms of two models (single force and moment tensor) at (A) CTA and (B) KON for Kalapana event. For each station, top two, middle two, and bottom two pairs of seismograms are vertical, radial, and transverse components, respectively. For each two pairs of traces, the top and the bottom pairs are for CSF and CMT solutions, respectively.

TABLE 3. CMT Solutions (4-5 mHz) for Kalapana

Centroid location			
Time		+34.1 s	
Latitude, longitude		−0.5°, −0.2°	
Depth		10 km	
Moment tensor		(10^{19} N m)	
M_{rr}		7.01 ± 0.18	
$M_{\theta\theta}$		-6.30 ± 0.23	
$M_{\phi\phi}$		-0.71 ± 0.19	
$M_{r\theta}$		7.27 ± 1.21	
$M_{r\phi}$		10.33 ± 1.21	
$M_{\theta\phi}$		-2.25 ± 0.18	
Principal axes	Moment	Plunge	Azimuth
T-axis	15.28	56°	294°
N-axis	-1.79	13°	44°
P-axis	-13.49	31°	142°
Best double-couple			
moment		14.4	
strike1		41°	
dip1		77°	
strike2		267°	
dip2		19°	
Non double-couple		ε = 0.12	
Double couple inversion			
moment		12.5	
strike1		57°	
dip1		73°	
strike2		264°	
dip2		19°	

*Centroid time is relative to 1447:40.4.
**Centroid location is relative to 19.333°N, −155.033°E.

Furumoto and Kovach [1979]. The inversion converged to a shallow depth even without fixing the depth. The CMT centroid location is also very close to the epicentral location given by the Hawaii Volcano Observatory (HVO), while the CSF centroid is shifted by almost 2°. Table 4 compares variance reductions of the CSF and the CMT inversions for the three events studied in this paper. For the Kalapana event, the variance reduction of the CMT inversion is better than that of the CSF inversion, while for the other two events the situation is reversed, even though the number of parameters is smaller for the CSF inversion than for the CMT inversion.

It appears, therefore, that as far as the overall fit of the waveforms is concerned, a double couple model (i.e., CMT solution) explains the Kalapana event better than a single force model does. The CMT solution obtained here, however, still does not explain the large amplitude of the Love waves at the nodal directions for Rayleigh wave excitation, which led *Eissler and Kanamori* [1987, 1988] to propose a single force model. We may have to invoke a superposition of both types of

TABLE 2. CSF Solutions (4-5 mHz) for Kalapana

Data	M_{CSF} (10^{15} kg m)	Azimuth, deg	Plunge, deg	Latitude, deg	Centroid Longitude, deg	Time, s
All	339±30.	331.0±03.9	-22.9±03.2	+1.73	-1.08	29.7
ANMO	237±48.	316.0±14.4	-34.0±11.7	-0.14	-0.24	19.1
ALQ	230±70.	323.0±09.2	-30.4±11.2	-0.27	-0.50	26.6
CTA	338±58.	346.0±07.1	-24,3±06.1	+0.37	+0.65	30.8
KON	589±65.	332.8±07.2	-01.6±03.9	+1.57	+0.23	31.5
MAT	409±70.	319.6±15.8	-27.6±08.2	+0.57	-0.98	38.4
OGD	113±44.	272.6±48.9	55.1±26.6	-0.21	-0.29	27.6
ZLP	290±72.	326.9±17.4	-30.7±11.2	+0.31	-1.13	30.1

Centroid location is relative to 19.333°N, −155.033°E, and centroid time is relative to 1447:40.4, reported by HVO.

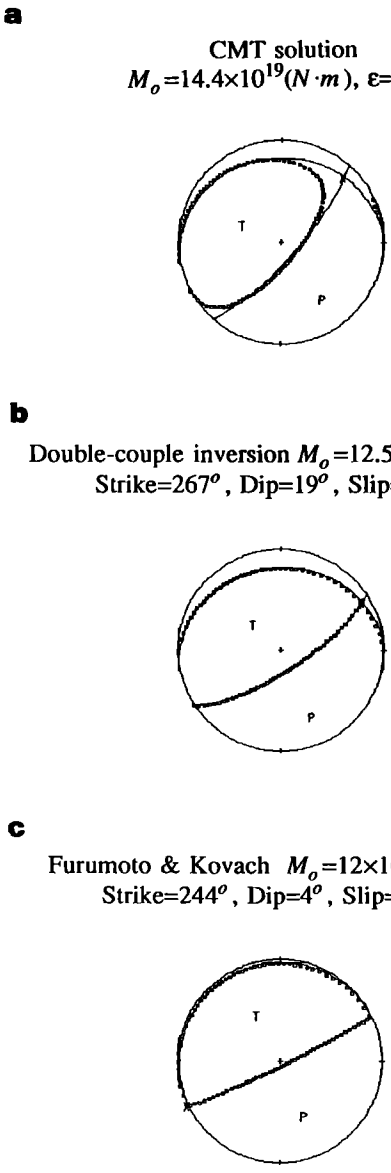

Fig. 8. Comparison of focal mechanism solutions. (A) The CMT solution. (B) The CMT solution with double-couple constraint. (C) The solution of *Furumoto and Kovach* [1979].

mechanism to explain this event. Although we have tried simultaneous inversion for a linear combination of CSF and CMT solutions, we could not obtain a stable solution. This is because these two representations of a seismic source are strongly linearly dependent. A more detailed analysis of this controversial event will be presented elsewhere (H. Kawakatsu and H. Kanamori, manuscript in preparation, 1989).

TABLE 4. Variance Reduction

	CSF	CMT
St. Helens	51%	47%
Kalapana	50%	66%*
Mantaro	40%	34%

The variance reduction is defined by

$$\frac{1}{N_s}\sum_{\text{all data}}^{N_s}[1-\int(u_o(t)-u_c(t))^2dt/\int u_o^2(t)dt]\times 100.$$

*64% for a double-couple inversion.

Mantaro Landslide, Peru, April 24, 1974

One of the largest historically recorded landslides occurred in the Mayunmarca valley (12.6°S, 74.6°W), adjacent to the Mantaro River, in the Peruvian Andes on April 25, 1974 [*Berrocal et al.*, 1978]. This event was, at the time, considered the largest historically recorded in the Western Hemisphere [*Kojan and Hutchinson*, 1978]. As far as the excitation of long period seismic waves is concerned, however, this event turns out to be only one tenth the size of the Mount St. Helens landslide.

The rockslide-avalanche traveled along the Mayunmarca Valley in the direction 45°E of North. *Kojan and Hutchinson* [1978] state that "the volume of slide material is approximately 10^9 m^3,...The maximum length of the slide, measured on the slope, is approximately 8.25 km. ... Along its central axis, the upper portion of the flow has a surface slope of 25°, reducing to 9½° downstream of the site of the town of Mayunmarca. Sideslopes, along which the initial rockslide occurred, are approximately 35°. ..."

Eight HGLP stations were operational at the time (Figure 9). Among them, all of the components at MAT and the horizontal components of OGD were too noisy to be used for inversion. We use data between 6 and 8 mHz, because longer period waves were not excited well. As the origin time of the landslide, we use 0157:22.5 UTC on April 26, 1974, calculated from P-arrival times from the HUA (epicentral distance of 82 km) short-period seismograms by *Berrocal et al.* [1978].

The CSF solution with the full data set indicates a direction of the force 49° west of south (Table 5 and Figure 10), and the CSF vector plunge is 7.3° (±2°) upward. These values are consistent with the observed direction of the landslide. The centroid time is about 60 s. If we assume that this also represents the half duration of the source function, the CSF value 1.33×10^{15} (kg m) should be multiplied by 1.62 to correct for the effect of source finiteness. The static (zero frequency) CSF value, then, becomes 2.2×10^{15} (kg m), which is about 10 times smaller than that of the Mount St. Helens landslide.

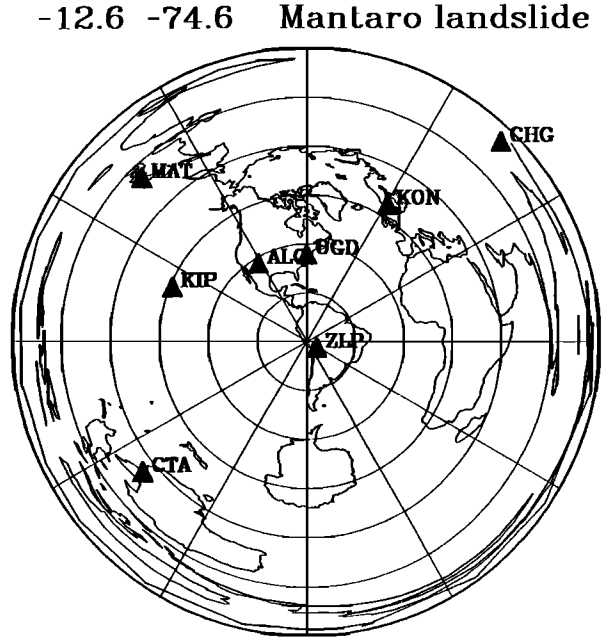

Fig. 9. The station coverage for the Mantaro landslide.

TABLE 5. CSF Solutions (6-8 mHz) for Mantaro

Data	M_{CSF} (10^{15} kg m)	Azimuth, deg	Plunge, deg	Centroid Latitude, deg	Centroid Longitude, deg	Time,s
All	1.40±0.12	229.0±02.6	-7.8±02.1	+0.54	+0.12	63.2
ALQ	1.64±0.56	216.9±13.1	-28.2±11.7	+1.05	-0.66	81.0
CHG	1.22±0.19	223.6±07.4	-4.9±07.4	+0.46	+0.46	60.2
CTA	1.21±0.38	214.5±37.4	4.8±10.2	+0.26	+0.33	56.2
KIP	1.31±1.80	200.9±24.7	5.7±19.2	+1.10	-2.75	131.4
KON	1.84±0.29	221.0±11.0	-33.7±08.6	+0.64	+0.39	63.6
ZLP	1.72±0.25	224.4±0.26	-5.9±01.8	+0.07	-0.11	65.7

Centroid location is relative to −12.6°N, −74.6°E, and centroid time is relative to 0157:22.5, taken from *Berrocal et al.* [1978].

The total volume of the slide material is approximately 10^9 m^3 [*Berrocal et al.*, 1978; *Kojan and Hutchinson*, 1978] which is about half of that of the Mount St. Helens event. The average distance that the centroid of the rockslide-avalanche traveled is about 4-6 km, which is about the same as the Mount St. Helens' landslide. However, the CSF value for the Mantaro landslides appears to be about 5 times smaller than the value expected from the observed travel distance and the volume of the rockslide-avalanche. This discrepancy suggests either that most of the rockslides moved aseismically or that the total volume of the slides was overestimated. Figure 11 compares the observed and synthetic seismograms.

DISCUSSION

Single Couple Source?

In the CSF inversion, we have neglected the effect of the seismic wave excitation due to a nearly vertical "single couple" source, which can be caused by loading and unloading of materials at the head and tail of the slide, respectively. Approximating the slide as a rigid block sliding on a horizontal surface at a speed v, the excitation due to this single couple force can be expressed in terms of $\dot{\Gamma}(t)$ in (9) as

$$\dot{\Gamma}^{sc}(t) \approx -Mg\frac{\partial(v(t)t)}{\partial t}\cdot\nabla_h u_r^* \qquad (15)$$

where u_r denotes the radial component of the eigenvector and the superscript "sc" signifies the "single couple" source.

If we take a sinusoidal source time function with a half duration τ for the effective single force $f^e(t)=\kappa Mg\sin(\pi t/\tau)$ (κ <1) [*Kanamori et al.*, 1984], the excitation becomes

$$\dot{\Gamma}^{sf}(t) \approx \kappa Mg\frac{\pi}{\tau}\cos(\frac{\pi}{\tau}t)u^* \qquad (16)$$

From (3), v(t) may be expressed as

$$v(t) = \kappa g\frac{\tau}{\pi}(1-\cos(\frac{\pi}{\tau}t)) \qquad (17)$$

Noting the scaling relation $|\nabla_h u_r| \approx l u_h/a$, where l and a are the angular order and the radius of the Earth, the average ratio of the two excitation coefficients may be written as

$$R = <\frac{|\dot{\Gamma}^{sc}|}{|\dot{\Gamma}^{sf}|}> \approx \frac{3\tau^2}{2\pi}g\frac{l}{a} \qquad (18)$$

If we take l = 40 (~212 s), then $R \approx \tau^2/3.4\times10^4$, and

$$R = \begin{cases} \frac{1}{4.2} & \text{for } \tau = 90 \text{ s} \\ \frac{1}{9.5} & \text{for } \tau = 60 \text{ s} \\ \frac{1}{38.} & \text{for } \tau = 30 \text{ s} \end{cases} \qquad (19)$$

The Rayleigh wave radiation pattern due to this couple force (it does not excite Love waves) is the same as that due to a horizontal single force and their polarities are opposite while the slide is accelerating and the same while it is decelerating.

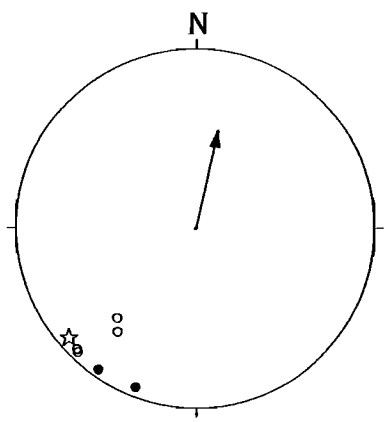

Fig. 10. Same as Figure 3 but for the Mantaro landslide.

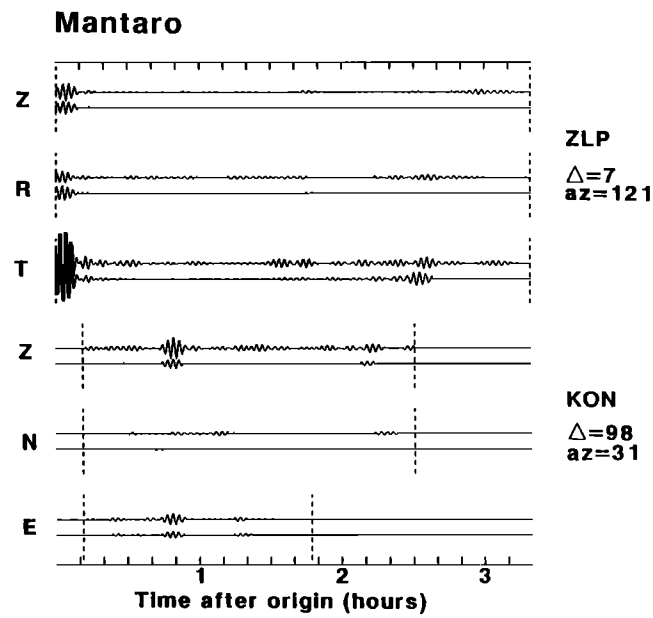

Fig. 11. Comparison of observed and synthetic seismograms at ZLP and KON for the Mantaro landslide. See Figure 4 caption for explanation.

For the case of the Mount St. Helens event, since τ=90 s, neglecting the single couple source may introduce some error (<25%) in Rayleigh wave waveform fitting. For the rest of the events, the assumption that the vertical couple force is negligible appears to be reasonable.

Peak Acceleration

If we assume a sinusoidal time function for the effective force, we can express the peak acceleration κg in terms of the travel distance (D) and the total duration (2τ) of the slide:

$$\kappa g = \frac{\pi D}{2\tau^2}$$

Assuming that the peak acceleration is the component of the gravitational acceleration projected onto the direction of the slide, we can infer the slope of the slide (i.e., direction of the force) from D and τ. The inferred slopes for the Mount St. Helens and Mantaro events are 5.6° and 12.9°, respectively. These values are quite consistent with the estimated plunge of the CSF vectors, suggesting that the peak acceleration is actually the component of the gravitational acceleration projected onto the direction of the slide.

Table 6 compares the results of the three CSF inversions. As noted earlier, the CSF value for the Mantaro landslide is about 5 times smaller than that expected from the "observed" mass and travel distance, while for the St. Helens event they are quite consistent. Since the total duration of the Mantaro landslide appears to require the peak force to be the maximum possible force (i.e., the component of the gravitational force projected onto the slope), we may at least say that the mass of the slide which excited seismic waves should be about 5 times smaller than the mass that was "observed" geologically.

Centroid Locations

It is often noted that the epicentral centroid of the CMT inversion is mostly affected by the Earth's lateral heterogeneity and that the location itself does not have much significance [*Dziewonski et al.*, 1981; *Dziewonski and Woodhouse*, 1983]. This also appears to be the case for the CSF inversion, since the relative locations of the centroid to the reported epicenters do not show much correlation with the directions of the landslides. We, however, consider that the magnitude of the relative distance (say, δx) contains some information about how the model fits data. δx is smaller than 0.3° for most of events in the Harvard CMT solutions. δx can be larger in our case because we use much longer periods of data. Our experience suggests that when earthquakes (landslides) are modeled successfully by the CMT (CSF) method, δx is smaller than 1°. In the case of the St. Helens event, δx is 0.22° or the CSF inversion, while δx from CMT is larger than 2°. This occurs because the initial source phase of the surface wave excitation due to a landslide is different from that due to an earthquake faulting. We think that the adjustment of the unmodeled initial phases resulted in the large shift of the centroid location in the CMT inversion. Although more experience is necessary, the size of the centroid shift may be one way to discriminate a landslide from regular earthquakes.

The temporal centroid of the CSF inversion, instead, appears to be a good estimate of the half duration of the source time. This is so because landslides are very slow phenomena compared with regular earthquakes and the source durations are longer than a minute. The relative time shift of the centroid to the origin time for the St. Helens event is 103 s (Table 1), while *Kanamori and Given* [1982] estimated the half duration to be ~90 s; the centroid time shift of the CSF solution for the Mantaro landslide is 63 s (Table 5), while *Berrocal et al.* [1978] suggest the total duration to be longer than 90 s. We, therefore, consider that the centroid time shift of the CSF inversion can be a good first order estimate of the half duration time of a landslide.

Discriminating a Landslide From Regular Earthquakes

Table 4 compares the variance reductions of the CSF and CMT solutions for the events studied in the present paper. For those events which are known to be landslides, the variance reduction of the CSF solutions is larger than those of the CMT solutions, even though the number of parameters is less in the CSF inversion. The amount of the epicentral centroid shift can be also used to discriminate a landslide from earthquakes as suggested in the previous section.

Another way of discrimination is to look at the excitation spectra at long periods. The spectra excitation for landslides is fundamentally different from earthquakes in that the spectra levels fall off towards very low frequencies. This occurs because the characteristics of these two seismic source time functions are fundamentally different as discussed earlier and as shown in Figure 1. If broadband data are available and such spectrum fall-off at low frequencies are observed, it is likely that the seismic event is a landslide. Using broadband data, it will be then possible to deconvolve the source time function to estimate the momentum time history as *Kanamori et al.* [1984] tried for the St. Helens event. Unfortunately the network response of the HGLP stations, which are used to analyze the other two events, at low frequencies is not well known to allow us to estimate the momentum time histories.

Overlooked 'Seismic' Events

The Mantaro landslide was not identified as an earthquake in regular earthquake catalogues (e.g., the ISC bulletin), possibly due to its slow nature. Although there is a report of an earthquake with M_s=5.2, the main radiated seismic energy of the Mount St. Helens event is also missed in the catalogues. This

TABLE 6. Comparison of CSF Solutions

	M_{CSF} (10^{15} kg m)	Azimuth, deg	Plunge, deg	Time, s	Mass (10^{12} kg)	Distance, km	Expected M_{CSF}	Inferred Slope, deg
St. Helens	22.0	187	-5	103	4.6	5.0	23.0	5.6
Mantaro	2.2	229	-8	63	2.0	5.0	10.0	12.9
Kalapana	370.0	331	-23	30	10^3–10^4	37-370 m*	-	-

Density is assumed to be 2×10^3 kg/m^3.
*Calculated from the CSF value.

suggests that there may exist many such seismic events, especially under the oceans (e.g., suboceanic slumping), which have been overlooked by conventional "first motion" seismology.

As shown in the present work, we can now identify a landslide by analyzing waveform data obtained from the global digital seismic networks. In the near future, by analyzing waveform data obtained from global broadband digital seismic networks (e.g, the proposed POSEIDON network [*Japan National Committee for Seismology and Physics of the Earth's Interior*, 1987]) using methods like CMT inversion [*Dziewonski et al.*, 1981] or the method presented in the present paper, we may find many seismic events which might have been overlooked.

CONCLUSION

We have presented a new CSF waveform inversion method to analyze the long period seismic waves generated by gigantic landslides. We have applied this method to the 1980 Mount St. Helens event, the 1975 Kalapana earthquake, and the 1974 Mantaro landslide and the conclusions are as follows;

1. Mount St. Helens: The CSF solution is $M_{CSF}=15\times10^{15}$kg m, azimuth=187°, plunge=–5.2°, and is consistent with actual geological observations.

2. Kalapana earthquake: The CSF solution is $M_{CSF}=339\times10^{15}$kg m, azimuth=331°, plunge=–23°, but this does not fit the overall waveforms better than the CMT solution. The CMT solution, however, still does not explain the observed Love wave radiation pattern. We may therefore have to invoke a combination of a point moment tensor and landslide mechanisms for this event.

3. Mantaro landslide: The CSF solution is $M_{CSF}=1.4\times10^{15}$kg m, azimuth=229°, plunge=–7.8°. Although the geometry of the CSF solution (i.e., the direction of the force) is consistent with the actual landslide, the magnitude of the CSF value is about 5 times smaller than that expected from the observed mass and travel distance of the landslide. This discrepancy may suggest either a relatively aseismic nature of the landslide or that the total volume of the slide was overestimated.

4. Single station CSF inversion is possible and appears to be stable and useful.

The possibility of discriminating landslides from regular earthquakes in the future using broadband seismic waveforms is also discussed.

APPENDIX A

HGLP stations are the prototype of the current SRO and ASRO stations, and were operated at some stations since 1972. Although they have good sensitivity at long periods (>200 s), detailed calibration information is unfortunately not available. We use a response function tabulated by R. P. Comer. In his unpublished manuscript, he describes that "...Calibration sheets provided with the data gave the amplitude response for individual components on dates close to June 10, 1975 and some phase information was also available. Some secular drift of the gains was evident, but did not appear to be too severe. ..., we adopted the response of the vertical instrument as Albuquerque (ALQ-Z) for July 9, 1975 adopted as a standard..." Since the first SRO station, ANMO, was in operational at the time of the Kalapana event, as well as the HGLP ALQ station (both at Albuquerque, New Mexico), we could actually check the accuracy of the assumed instrument response by comparing two sets of deconvolved seismograms and they agreed quite well.

The calibration sheets, given us by J. Hoffman of the U.S. Geological Survey (Albuquerque, N.M.), show differences of amplitude response among different stations as well as different components at a same station. Above a period of 100 s, however, they are relatively stable and appear to be accurate within a error of 20-30%, except for some peculiar stations. We therefore think it is reasonable to use Comer's response function as the standard (shown in Table A1 and Figure A1).

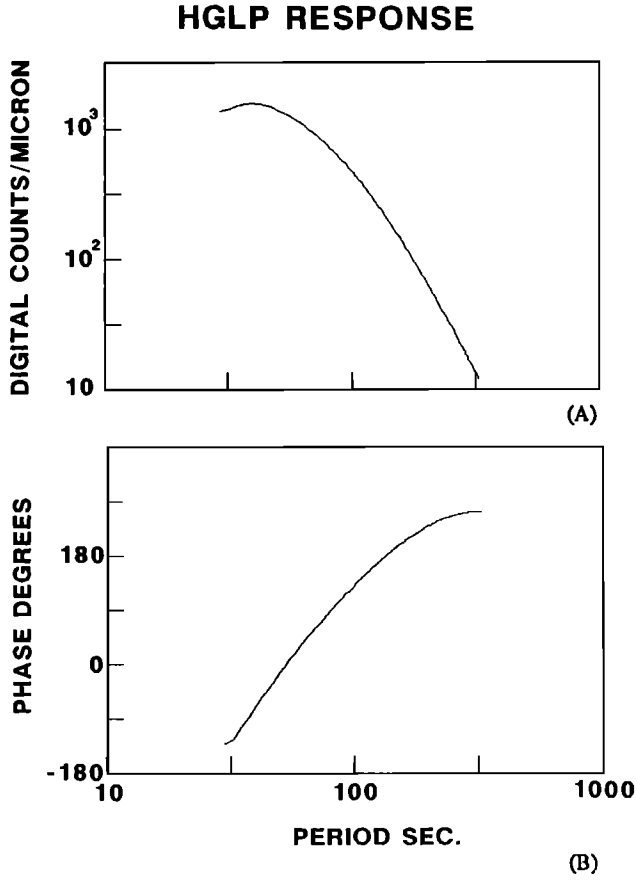

Fig. A1. Instrumental response function of HGLP station. (A) Amplitude. (B) Phase.

TABLE A1. HGLP Station Response

Period, s	Amplitude, digital counts/micron	Phase, rad
40.	1.56e+03	-1.20
60.	1.16e+03	0.50
80.	7.51e+02	1.55
100.	4.78e+02	2.29
120.	3.08e+02	2.84
140.	2.03e+02	3.26
160.	1.38e+02	3.59
180.	9.62e+01	3.84
200.	6.86e+01	4.03
220.	5.00e+01	4.18
240.	3.71e+01	4.28
260.	2.81e+01	4.35
280.	2.16e+01	4.40
300.	1.68e+01	4.43
320.	1.33e+01	4.44

APPENDIX B

TABLE B1. Expressions for Kernels

	i=1($\hat{r}$)	2($\hat{\theta}$)	3($\hat{\phi}$)
Ψ_{ij}^{lmq}			
j=1(r)	$\sigma_1 P_l^0$	$\sigma_2 \dot{P}_l^0$	0
2(θ)	$\sigma_3 P_l^1 \cos\phi$	$\left[\sigma_4 \dot{P}_l^1 + \frac{\sigma_9}{\sin\theta} P_l^1\right] \cos\phi$	$(-1)\left[\frac{\sigma_4}{\sin\theta} P_l^1 + \sigma_9 \dot{P}_l^1\right] \sin\phi$
3(φ)	$\sigma_3 P_l^1 \sin\phi$	$\left[\sigma_4 \dot{P}_l^1 + \frac{\sigma_9}{\sin\theta} P_l^1\right] \sin\phi$	$\left[\frac{\sigma_4}{\sin\theta} P_l^1 + \sigma_9 \dot{P}_l^1\right] \cos\phi$
B_{ij}^{lmq}			
1(r)	$\sigma_5 P_l^0$	$\sigma_6 \dot{P}_l^0$	0
2(θ)	$\sigma_7 P_l^1 \cos\phi$	$\left[\sigma_8 \dot{P}_l^1 + \frac{\sigma_{10}}{\sin\theta} P_l^1\right] \cos\phi$	$(-1)\left[\frac{\sigma_8}{\sin\theta} P_l^1 + \sigma_{10} \dot{P}_l^1\right] \sin\phi$
3(φ)	$\sigma_7 P_l^1 \sin\phi$	$\left[\sigma_8 \dot{P}_l^1 + \frac{\sigma_{10}}{\sin\theta} P_l^1\right] \sin\phi$	$\left[\frac{\sigma_8}{\sin\theta} P_l^1 + \sigma_{10} \dot{P}_l^1\right] \cos\phi$
C_{ij}^{lmq}			
1(r)	$(\sigma_1 - \sigma_3) P_l^1 \cos\phi$	$\left[(\sigma_2 - \sigma_4) \dot{P}_l^1 - \frac{\sigma_9}{\sin\theta} P_l^1\right] \cos\phi$	$\left[\frac{\sigma_4 - \sigma_2}{\sin\theta} P_l^1 + \sigma_9 \dot{P}_l^1\right] \sin\phi$
2(θ)	$(\sigma_1 - \frac{L^2}{2}\sigma_3) P_l^0$	$(\sigma_2 - \frac{L^2}{2}\sigma_4) \dot{P}_l^0$	$(-1)\left[\frac{\sigma_4}{\sin\theta} P_l^2 + \frac{\sigma_9}{2} \dot{P}_l^2\right] \sin 2\phi$
	$+\frac{\sigma_3}{2} P_l^2 \cos 2\phi$	$+\left[\frac{\sigma_4}{2} \dot{P}_l^2 + \frac{\sigma_9}{\sin\theta} P_l^2\right] \cos 2\phi$	
3(φ)	$\frac{1}{4}\sigma_3 P_l^2 \sin 2\phi$	$\left[\frac{1}{4}\sigma_4 \dot{P}_l^2 + \frac{\sigma_9}{\sin\theta} P_l^2\right] \sin 2\phi$	$\frac{1}{2}\left[\frac{\sigma_4}{\sin\theta} P_l^2 + \sigma_9 \dot{P}_l^2\right] \cos 2\phi$
D_{ij}^{lmq}			
1(r)	$(\sigma_1 - \sigma_3) P_l^1 \sin\phi$	$\left[(\sigma_2 - \sigma_4) \dot{P}_l^1 - \frac{\sigma_9}{\sin\theta} P_l^1\right] \sin\phi$	$(-1)\left[\frac{\sigma_4 - \sigma_2}{\sin\theta} P_l^1 + \sigma_9 \dot{P}_l^1\right] \cos\phi$
2(θ)	$\frac{1}{4}\sigma_3 P_l^2 \sin 2\phi$	$\left[\frac{1}{4}\sigma_4 \dot{P}_l^2 + \frac{\sigma_9}{\sin\theta} P_l^2\right] \sin 2\phi$	$\frac{1}{2}\left[\frac{\sigma_4}{\sin\theta} P_l^2 + \sigma_9 \dot{P}_l^2\right] \cos 2\phi$
3(φ)	$(\sigma_1 - \frac{L^2}{2}\sigma_3) P_l^0$	$(\sigma_2 - \frac{L^2}{2}\sigma_4) \dot{P}_l^0$	$\left[\frac{\sigma_4}{\sin\theta} P_l^2 + \frac{\sigma_9}{2} \dot{P}_l^2\right] \sin 2\phi$
	$-\frac{\sigma_3}{2} P_l^2 \cos 2\phi$	$-\left[\frac{\sigma_4}{2} \dot{P}_l^2 + \frac{\sigma_9}{\sin\theta} P_l^2\right] \cos 2\phi$	

$L = \sqrt{l(l+1)}$. P_l^m is an associated Legendre function, and an overdot denotes its θ derivative.

In (14) we have an expression for the seismic displacement field of the form

$$s_i(x,t) = \sum_{j=1}^{3} \psi_{ij}(t)P_i + \delta r_s b_i(t) + \delta\theta_s c_i(t) + \delta\phi_s d_i(t) + \Delta t e_i(t) \quad \text{(B1)}$$

where i=1,2,3 refer to the vertical, radial, and transverse components, respectively. $\psi_{ij}(t)$, $b_h(t)$, $c_h(t)$, $d_h(t)$, $e_h(t)$, can be written in the following form:

$$\psi_{ij}(t) = \sum_{lnq} \frac{2l+1}{4\pi} r_s \Psi_{ij}^{lnq}(t)$$

$$b_i(t) = \sum_{lnq} \frac{2l+1}{4\pi} B_{ij}^{lnq}(t) P_j$$

$$c_i(t) = \sum_{lnq} \frac{2l+1}{4\pi} r_s C_{ij}^{lnq}(t) P_j$$

$$d_i(t) = \sum_{lnq} \frac{2l+1}{4\pi} \frac{r_s}{\sin\theta} D_{ij}^{lnq}(t) P_j$$

$$\dot{e}_i(t) = \sum_{lnq} \frac{2l+1}{4\pi} r_s \dot{\Psi}_{ij}^{lnq}(t) P_j$$

where summations are done over angular order l, overtone number n, and mode type q (spheroidal or toroidal). The explicit expressions for $\Psi_{ij}^{lnq}(t)$, $B_{ij}^{lnq}(t)$, $C_{ij}^{lnq}(t)$, and $D_{ij}^{lnq}(t)$ are given in Table B1, where the σ are defined by

$$\sigma_1 = \sigma_1^{lnq} = r_s^{-1} U(r_s) U(a) h_k(t)$$

$$\sigma_2 = \sigma_2^{lnq} = r_s^{-1} U(r_s) V(a) h_k(t)$$

$$\sigma_3 = \sigma_3^{lnq} = r_s^{-1} V(r_s) U(a) h_k(t)$$

$$\sigma_4 = \sigma_4^{lnq} = r_s^{-1} V(r_s) V(a) h_k(t)$$

$$\sigma_5 = \sigma_5^{lnq} = U'(r_s) U(a) h_k(t)$$

$$\sigma_6 = \sigma_6^{lnq} = U'(r_s) V(a) h_k(t)$$

$$\sigma_7 = \sigma_7^{lnq} = V'(r_s) U(a) h_k(t)$$

$$\sigma_8 = \sigma_8^{lnq} = V'(r_s) V(a) h_k(t)$$

$$\sigma_9 = \sigma_9^{lnq} = r_s^{-1} W(r_s) W(a) h_k(t)$$

$$\sigma_{10} = \sigma_{10}^{lnq} = W'(r_s) W(a) h_k(t)$$

Acknowledgments. I am grateful to John Hoffman of the U.S. Geological Survey (Albuquerque) for supplying the HGLP data and to Hiroo Kanamori for showing me the paper by Berrocal et al. Toshiro Tanimoto kindly allowed me to use his normal mode solution set. Earlier conversations with Satoru Honda and Kiyoshi Yomogida on generalization of Backus and Mulcahy's paper and discussions with Hiroo Kanamori on single force sources were helpful in formulating the problem. I thank Bob Geller, Hiroo Kanamori, Keiko Kuge, and Kiyoshi Yomogida for carefully reading the manuscript and Göran Ekström and an anonymous reviewer for the constructive reviews. This work was supported by U.S. Geological Survey grant 14-08-0001-G1356. Contribution 4738, Division of Geological and Planetary Sciences, California Institute of Technology, Pasadena.

REFERENCES

Ando, M., The Hawaii earthquake of November 29, 1975: Low dip angle faulting due to forceful injection of magma, *J. Geophys. Res., 84*, 7616-7626, 1979.

Backus, G., Interpreting the seismic glut moments of total degree two or less, *Geophys. J. R. Astron. Soc., 51*, 1-25, 1977.

Backus, G., and M. Mulcahy. Moment tensors and other phenomenological descriptions of seismic sources, I, Continuous displacements, *Geophys. J. R. Astron. Soc., 46*, 341-361, 1976.

Berrocal, J., A. F. Espinosa, and J. Galdos, Seismological and geological aspects of the Mantaro landslide in Peru, *Nature, 275*, 533-536, 1978.

Burger, R. W., and C. A. Langston, Source mechanism of the May 18, 1980, Mount St. Helens eruption from regional surface waves, *J. Geophys. Res., 90*, 7653-7664, 1985.

Dziewonski, A. M., and J. H. Woodhouse, Studies of the seismic source using normal-mode theory, *in Earthquakes: observation, theory and interpretation*, edited by H. Kanamori, and E. Boschi, pp. 45-137, North-Holland, Amsterdam, 1983.

Dziewonski, A. M., T.-A. Chou, and J. H. Woodhouse, Determination of earthquake source parameters from waveform data for studies of global and regional seismicity, *J. Geophys. Res., 86*, 2825-2853, 1981.

Eissler, H. K., and H. Kanamori, A single-force model for the 1975 Kalapana, Hawaii, earthquake, *J. Geophys. Res., 92*, 4827-4836, 1987.

Eissler, H. K., and H. Kanamori, Reply, *J. Geophys. Res., 93*, 8083-8084, 1988.

Ekström, G., A. M. Dziewonski, and J. M. Steim, Single station CMT; application to the Michoacan, Mexico, earthquake of September 19, 1985, *Geophys. Res. Lett., 13*, 173-176, 1986.

Furumoto, A. S., and R. L. Kovach, The Kalapana earthquake of November 29, 1975: An intra-plate earthquake and its relation to geothermal processes, *Phys. Earth Planet. Inter., 18*, 197-208, 1979.

Gilbert, F., and A. M. Dziewonski, An application of normal mode theory to the retrieval of structural parameters and source mechanisms from seismic spectra, *Philos. Trans. R. Soc. London, Ser. A, 278*, 187-269, 1975.

Hasegawa, H. S., and H. Kanamori, Source mechanism of the magnitude 7.2 Grand Banks earthquake of November 1929: double couple or submarine landslide? *Bull. Seismol. Soc. Am., 77*, 1984-2004, 1987.

Japan National Committee for Seismology and Physics of the Earth's Interior, POSEIDON (Pacific Orient Seismic Digital Observation Network), 16pp., Global Seismology Subcommittee, Tokyo, 1987.

Kanamori, H., and J. W. Given, Analysis of long-period seismic waves excited by the May 18, 1980, eruption of Mount St. Helens: A terrestrial monopole, *J. Geophys. Res., 87*, 5422-5432, 1982.

Kanamori, H., J. W. Given, and T. Lay, Analysis of seismic body waves excited by the Mount St. Helens eruption of May 18, 1980, *J. Geophys. Res., 89*, 1856-1866, 1984.

Kojan, E., and J. N. Hutchinson, Mayunmarca rockslide and debris flow, Peru, *in Rockslides and Avalanches-1, Natural phenomena*, edited by B. Voight, pp. 315-361, Elsevier, Amsterdam, 1978.

Lipman, P. W., J. P. Lockwood, R. T. Okamura, D. A. Swanson, and K. M. Yamashita, Ground deformation associated with the 1975 magnitude-7.2 earthquake and resulting changes in activity of Kilauea volcano, Hawaii, *U.S. Geol. Surv. Prof. Pap., 1276*, 45 pp., 1985.

Sipkin, S. A., Estimation of earthquake source parameters by the inversion of waveform data: global seismicity, 1981-1983, *Bull. Seismol. Soc. Am., 76*, 1515-1541, 1986.

Voight, B., H. Glicken, R. J. Janda, and P. M. Douglass, Catastrophic rockslide-avalanche of May 18, the 1980 eruptions of Mount St. Helens, *U.S. Geol. Surv. Prof. Pap., 1250*, 347-378, 1981.

Wyss, M., and R. L. Kovach, Comment on "A single-force model for the 1975 Kalapana, Hawaii, earthquake" by Holly K. Eissler and Hiroo Kanamori, *J. Geophys. Res., 93*, 8078-8082, 1988.

H. Kawakatsu, Geological Survey of Japan, 1-1-3 Higashi, Tsukuba, Ibaraki 305, Japan.

(Received February 1, 1989;
revised May 26, 1989;
accepted June 2, 1989)